Received: 14 February 2022 | Revised: 25 March 2022 | Accepted: 28 March 2022

DOI: 10.1002/cjce.24535

SPECIAL ISSUE ARTICLE

THE CANADIAN JOURNAL OF CHEMICAL ENGINEERING

Steam reforming of tar in hot syngas cleaning by different catalysts: Removal efficiency and coke layer characterization

Francesco Parrillo[1] | **Carmine Boccia**[1,2] | **Giovanna Ruoppolo**[3] | **Mario Commodo**[3] | **Franco Berruti**[2] | **Umberto Arena**[1]

[1]Department of Environmental, Biological, Pharmaceutical Sciences and Technologies (DISTABIF), University of Campania Luigi Vanvitelli, Caserta, Italy

[2]Institute for Chemicals and Fuels from Alternative Resources (ICFAR), Western University, London, Ontario, Canada

[3]Institute of Sciences and Technologies for Sustainable Energy and Mobility (STEMS), National Research Council-CNR, Naples, Italy

Correspondence
Francesco Parrillo, Department of Environmental, Biological, Pharmaceutical Sciences and Technologies (DISTABIF), University of Campania Luigi Vanvitelli, Via Vivaldi, 43, 81100, Caserta, Italy.
Email: francesco.parrillo@unicampania.it

Abstract

Syngas produced by biomass and waste gasification processes must be adequately clean of tar compounds before being utilized in value-added applications. Syngas cleaning by tar cracking at high temperatures is a promising technique that can utilize different kinds of catalysts. However, their use is limited by the deposition of coke layers, which induces a masking phenomenon on the active surface, and, consequently, the rapid deactivation of the catalyst. This study addresses how the temperature (750 and 800°C) and the steam concentration (0% and 7.5%) can affect the extent of water–gas and reforming reactions between steam and coke deposits. Two catalysts were used: a market-available activated carbon and an iron-based alumina catalyst. The tests showed better performance of the Fe/γ-Al_2O_3 catalyst. A mass increase of the bed was measured in tests with both the catalysts, which confirms the deposition of the coke layer produced by tar dehydrogenation and carbonization. Scanning electronic microscopy-energy-dispersive X-ray analysis (SEM-EDX) and Raman spectroscopy were utilized to investigate the nature of coke layers over the catalyst surface, with the aim of acquiring information about their reactivity towards the water gas reaction. SEM-EDX observations indicate that the thickness of these carbon layers is less than 2 μm. Raman spectra suggest a negligible effect of the reaction temperature in the tested range and, in particular, that the amorphous nature of coke layers deposited in the presence of steam is relatively more graphitic than that obtained without steam.

KEYWORDS

coke deposition, Raman spectroscopy, steam reforming, syngas cleaning, tar cracking

1 | INTRODUCTION

The gasification process converts a solid or liquid carbon-based material into gaseous products using different types of gasifying agents.[1,2] The obtained fuel gas, called syngas, is mainly composed of H_2, CO, small amounts of CH_4, and inorganic and organic impurities that have to be removed to allow syngas utilization as an energy carrier or as a precursor for the synthesis of fuels and chemicals. Among these impurities, tars represent the greatest obstacle to the commercial expansion of the gasification processes.[1,3] Tars are a mixture of a wide range of heavy hydrocarbons that, due to their high dew point (higher than 350°C), can condense along pipes and within downstream equipment, leading to serious problems, such as blockages, corrosion, and syngas chemical energy loss. This necessarily implies plant shutdown, increasing operating costs and reducing the overall efficiency of the process.[4] Syngas cleaning methods for tar removal can be classified into primary methods, applied inside the gasifier through specific design solutions and the careful control of the reactor operating conditions, and secondary methods, applied downstream of the reactor. Currently, all secondary methods, despite the high tar conversion efficiencies, show economic and technical limits that prevent their full commercial utilization. Among them, the tar catalytic cracking at high temperatures allows to covert tars and preserve their chemical energy. It is generally known[5] that this hot syngas cleaning method suffers from deactivation phenomena due to metal sintering and/or coke deposition.

The former can be avoided through the use of resistant supports, such as activated carbons (AKs).[6] Moreover, due to their high surface area, high pore volume, thermal stability, and availability of oxygen-containing functional groups and inorganic elements, AKs could act as catalysts.[7–10] They are also relatively low-cost, easily available, and can be specifically prepared starting from coal or biomass.[11] The first studies on tar conversion by the means of AKs[12–15] measured high tar removal efficiencies, comparable to those obtained by using nickel-based catalysts, especially at temperatures above 800°C. A fundamental role is attributed to their specific surface area[16–18] and to the presence of inorganic elements.[19,20] Liu et al.[21] and Ashok et al.[5] demonstrated that the presence of O-functional groups positively affects the tar removal, probably because they play a role of active intermediates during the process.

The second, and more important, deactivation phenomenon is due to coke deposits on the catalyst surface, caused by tar dehydrogenation and carbonization. The conversion and removal of these coke layers could be achieved by using steam to trigger both tar and coke reforming reactions into light gases (H_2, CO, and CO_2), according to the water–gas (WG), water–gas shift (WGS), and steam reforming reactions.[22] Figure 1 reports possible, simplified, cracking and reforming mechanisms occurring to a tar model compound when it comes into contact with an appropriate catalyst.

An optimization of this possible cracking and reforming process needs an adequate characterization of the coke deposits, which is not an easy task when a carbonaceous catalyst, such as commercial AK, is used, as it is difficult to distinguish between the structure of the catalyst and that of the coke deposited on the surface.[23] Conversely, the coke deposition on non-carbonaceous supports[24] allows to avoid this problem. The most common catalysts used in the reforming processes of hydrocarbons are those composed of a metal oxide supported by Al_2O_3.[6,25] Metal oxides are a class of inorganic materials having a strong base surface terminating with O^{2-} ions.[26] Among the different metals used in reforming processes, iron appears to be the most commonly used, since it offers a low-cost alternative to the other catalytic metals[27] and has good capability and reliability to the loading and dispersion on catalyst support.[28] Al_2O_3 is a ceramic material that has good hardness, high melting point, and low electrical conductivity. In catalysis, its γ-form is the most widely used support due to the high mechanical strength, relatively high surface area, basic and acidic strength, and low-cost of production.[29] The catalytic activity of alumina is related to the complex mixture of aluminum, oxygen, and hydroxyl ions that are combined in ways to produce both acid and base sites.[30] Metal oxides supported by Al_2O_3 are also deactivated by coke formation, and, for this reason, several research groups studied its formation and characteristics by varying different parameters, such as the type of the tar model, the active sites, and the support.[24,31,32] These studies demonstrate that coke deposition is unavoidable during any tar removal process, both on carbonaceous and non-carbonaceous catalysts. Therefore, in order to limit (or to possibly avoid) the catalyst deactivation, it is necessary to better investigate the nature of these deposits as well as their evolution under different operating conditions.

In this framework, this paper uses naphthalene as a model tar compound and compares its removal efficiency using a commercial AK with that of a non-carbonaceous catalyst (Fe/γ-Al_2O_3) by means of a series of long-term tests. The research focused on the catalyst removal efficiencies and the characterization of the coke layer deposit, under different values of process temperatures and steam concentrations. Various diagnostic techniques, such as gas chromatograph-mass spectrometry (GC-MS), gas chromatograph-thermal conductivity

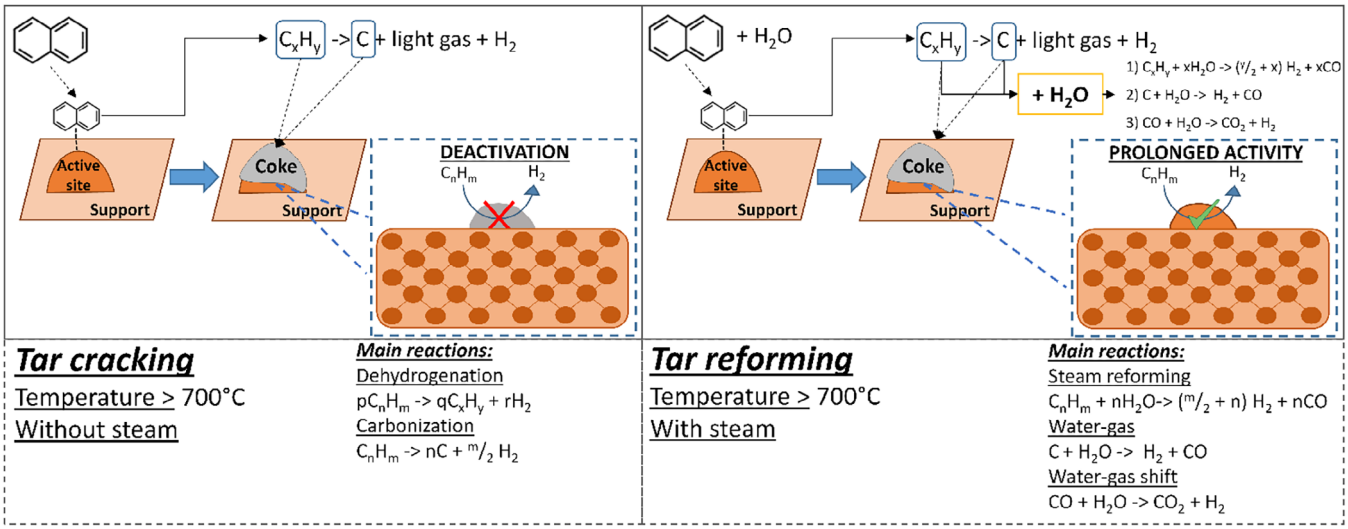

FIGURE 1 Simplified cracking and reforming mechanisms for a tar model compound on a catalyst

detection (GC-TCD), porosimetric analysis, scanning electronic microscopy (SEM) with energy-dispersive X-ray analysis (EDX), and Raman spectroscopy were utilized. The aim is to increase the knowledge of the chemical and morphological nature of coke deposits and suggest ways to improve catalyst tar removal performance.

2 | MATERIALS AND METHODS

2.1 | Tar model compound and selected catalysts

Naphthalene ($C_{10}H_8$) was used as a tar model compound since it is recognized as the most common and stable hydrocarbon in a tar mixture obtained from different types of gasification processes.[1,18,33,34] Two different catalysts have been used for the tests: an AK and a non-carbonaceous catalyst. The first is produced by Cabot© and is commercialized as Norit RB4W (Table 1). It is a coal-derived AK suitable for hot syngas applications at temperatures above 700°C, having surface area and pore volume equal to 928 m^2/g and 0.51 cm^3/g, respectively.[18,20,23] The second is a previously developed Fe catalyst supported on commercial γ-Al_2O_3 spheres,[35] produced by Sasol Germany GmbH© (Table 2). An iron content of 3 wt.% was added by dissolving the corresponding amount of iron nitrate $Fe(NO_3)_3 \cdot 9H_2O$ (98+%, Sigma-Aldrich) in aqueous solution and by adding a suitable amount of support. The material was then dried at 120°C for 12 h and calcined at 800°C with air. The iron addition did not remarkably affect the support properties since the resulting surface area and pore volume were 147 m^2/g and 0.47 cm^3/g, respectively.

2.2 | Experimental and diagnostic apparatus

The tests were carried out using a bench-scale vertical tubular quartz reactor with an internal diameter of 14 mm and a total height of 600 mm, described in detail in previous studies.[18,23] Nitrogen was used as an inert carrier gas and fed to two bubblers each containing 20 g of solid naphthalene. These bubblers were immersed in an oil bath kept at 65°C to obtain a constant tar model concentration of 22.5 mg/L_N. Water was introduced by the means of a peristaltic pump and vaporized in a 15 cm long heat exchanger, kept at 150°C. The steam was mixed with nitrogen and naphthalene before entering the reactor. All the lines were heated at 150°C to avoid gas condensation. At the reactor outlet, the gas was directed to a cleaning section or to a sampling section, by switching a three-way valve. The sampling section consists of three bubblers containing 2-propanol at 0°C, used for sampling of the residual naphthalene in the gas flow. During the remaining part of the test, the gas was sent to the cleaning section, which consists of an oil bubbler, for the removal of any impurities. The two sections are connected to a gas chromatograph equipped with a thermal conductivity detector (GC-TCD), capable of measuring the concentrations of H_2, CO, CH_4, N_2, CO_2, and low-molecular-weight hydrocarbons. The sampled tar collected in the bubblers was analyzed by a gas chromatograph coupled with a mass spectrometer (GC-MS Agilent HP6890/HP5975). The measurements of catalyst surface area were obtained by a Quantachrome Autosorb 1-C analyzer according to the Brunauer–Emmett–Teller (BET) method by N_2 adsorption at 77 K. Adsorption/desorption data were processed to evaluate the pore size

TABLE 1 Characterization of the tested activated carbon (AK) granules

Proximate analysis ($\%_{drybasis}$)		Ultimate analysis ($\%_{drybasis}$)		Inorganic fraction analysis ($mg/kg_{drybasis}$)	
Volatile matter	6.34	Carbon	85.89	Na	57.2
Fixed carbon	84.55	Hydrogen	0.21	K	58.2
Ash	9.11	Nitrogen	0.57	Mg	89.2
		Oxygen	4.22	Ca	331
Physical properties		Ash	9.11	Al	400
Diameter (mm)	0.8–1.2			Fe	297
Surface area (m^2/g)	928			Si	626
Pore volume (cm^3/g)	0.51			Cu	0.8

Abbreviation: AK, activated carbon.

TABLE 2 Characterization of the commercial γ-Al_2O_3 spheres

Physical properties		Inorganic fraction analysis (%)[a]	
Crystal structure	γ-phase	Al_2O_3	>97
Diameter (mm)	0.9–1.1	Si	0.020
Crush strength (N)	>45	Fe	0.015
Packed bulk density (g/dm^3)	740–820	Ti	0.015
Surface area (m^2/g)	150–170	Na	0.002
Pore volume (cm^3/g)	>0.45		

[a]Supplied by Sasol Germany GmbH©.

distribution in accordance with the density functional theory (DFT) and Monte-Carlo simulation method (DFT Kernel). SEM-EDX analyses of the different catalysts were carried out by means of a Field Electron and Ion (FEI) Inspect™ S50 SEM. Raman measurements of the catalysts before and after the tests were performed on a Raman microscope (Horiba XploRA) equipped with a 50 × objective (NA0.9, Olympus). The laser source was an Nd:YAG laser ($\lambda = 532$ nm, 12 mW maximum laser power at the sample). Three spots were randomly selected over the catalyst granules to verify the homogeneity of the samples. Finally, the acquired Raman spectra were baseline subtracted, normalized on the G band (~1580 cm^{-1}), and averaged for each sample analyzed.

2.3 | Experimental procedure and operating conditions tested

Both the catalysts were tested without and with the presence of steam at a concentration of 7.5%, at temperatures of 750 and 800°C. To keep the bed height and the gas residence time constant (0.11 s), 1.3 g of AK or 2.6 g of Fe/γ-Al_2O_3 were loaded before each respective test. The reactor with the bed was heated up to the selected experimental temperature under an inert atmosphere and kept at that temperature for 5 min. The peristaltic pump was calibrated before each test for 30 min. When the system reached a steady state, the nitrogen flow was sent to the naphthalene saturator and then to the reactor. Table 3 reports the experimental conditions for all the tests performed. After 5 min from the starting time, the first naphthalene sample was collected to determine the initial conversion efficiency of the catalyst bed. Further samples were collected every 30 min for the first two hours of testing, and then every hour until the end of the test. All the tests lasted a minimum of 6 h, except those performed with AK and without steam, where no gas species could be measured after 4 h. At the end of each test, the reactor was purged with N_2 atmosphere and allowed to cool down to room temperature. The tests measured the evolution over time of the gaseous species (monitored by the GC-TCD), the naphthalene conversion, the evolution of the porosimetric structure at different test conditions, and the evolution of the coke amorphous nature. A more detailed description of the apparatus and experimental procedure can be found in Boccia et al.[23]

3 | RESULTS AND DISCUSSION

The performance of the catalysts was tested at different temperatures (750 and 800°C) and steam concentrations (0% and 7.5%) while keeping all the other operating

TABLE 3 Operating parameters of the experimental tests performed on the NORIT RB4W and on the Fe/γ-Al_2O_3. All the tests have been repeated three times

($C_{10}H_8$) (mg/L_N)	22.5			
Residence time (s)	0.11			
T reactor (°C)	750		800	
T inlet (°C)	150		150	
$Q_{vol.}$ total (L_N/min)	0.49		0.47	
Nitrogen (vol.%)	100	92.5	100	92.5
Steam (vol.%)	0	7.5	0	7.5
$Q_{vol.}$ nitrogen (L_N/min)	0.49	0.45	0.47	0.45
$Q_{vol.}$ steam (L_N/min)	0	0.04	0	0.04

conditions fixed. The results are reported in terms of time evolution of gas composition, catalyst mass variation, naphthalene conversion efficiency, porosimetric analysis, SEM-EDX, and Raman analyses.

3.1 | Time evolution of gas composition

Figure 2 shows the evolution of the composition of the gases (H_2, CO, CO_2, and CH_4) generated during the tests with Fe/γ-Al_2O_3, as they were measured by the GC-TCD. Hydrogen production is the main index of naphthalene conversion, as it is the main product of all the cracking and reforming reactions, even though small concentrations of CO and CO_2 were also detected (Figure 1). Tests carried out without steam, at 750°C, show that H_2 concentration decreased in the first 2 h of testing and then remained constant at about 0.3%. At 800°C, this trend changed, with a constant decrease until complete deactivation was attributed to coke deposition. Tests carried out with steam show that the H_2 but also CO and CO_2 concentrations greatly increase with steam due to steam reforming, WG, and WGS reactions. At 800°C (and 7.5% of steam), the presence of a detectable CH_4 concentration was also identified. These results suggest the possible reforming of naphthalene into lighter hydrocarbons or the possible (even though rather limited) activation of the methanation reaction. Finally, the temperature increase leads to a higher yield of all gases in tests with steam, according to the endothermic nature of the reactions involved.

Figure 3 compares data obtained in tests with AK[23] with those obtained using Fe/γ-Al_2O_3. Without steam, the initial high H_2 concentrations were rather similar, as well as the subsequent rapid decrease, suggesting similar catalyst deactivation phenomena. On the contrary, during the tests with steam, the reforming reactions were strongly enhanced when using Fe/γ-Al_2O_3, resulting in higher concentrations of H_2. For instance, at a temperature of 750°C and a steam concentration of 7.5%, the presence of steam has no significant effect on H_2 production during tests with AK, whereas a clearly higher H_2 concentration (always higher than 1%) was detected with Fe/γ-Al_2O_3. Moreover, considerable CO and CO_2 concentrations were detected, which were almost absent in tests with AK.

For both Fe/γ-Al_2O_3 and AK, an unsteady trend of the outgoing gases was recorded, characterized by the presence of discontinuous peaks. This non-monotonous trend could be related to a discontinuous supply of steam from the peristaltic pump. Anyway, it is noteworthy that as the temperature increases, the peaks tend to increase in terms of frequency and maximum concentration reached. This suggests that another possible explanation is the periodic removal of the coke (or the structural carbon in the case of AK) that accumulates on the catalyst active sites and is then converted by the gasifying effect of the steam.

3.2 | Mass variation of the catalysts

The mass of catalysts was measured at the beginning (m_{INdev}) and at the end of each test (m_{OUT}). The variation per unit time was calculated using Equation (1) to enable comparison of tests having different durations.[9]

$$\Delta_{wt.}, \text{mg/min} = \frac{(m_{OUT}) - (m_{INdev})}{(t_{tot})} \quad (1)$$

Figure 4 reports the results obtained for both the catalysts at 750 and 800°C, with and without steam. All the tests show a mass increase of the catalysts bed in the reactor, that is, a $\Delta_{wt.}$ variation >0 mg/min, attributed to the deposition of the coke layer produced by tar dehydrogenation and carbonization, with the consequent masking of the catalytic sites. The situation changes by adding steam, leading to a significant reduction (more than 50% in most cases) of the mass gain for both the catalysts. This is due to the WG and reforming reactions occurring on the carbon layer covering the catalyst surface.

The Fe/γ-Al_2O_3 always shows the largest mass increase compared to the AK. This could be due to the result of two synergic factors: (a) without steam, wherein the greater accumulation of coke on the Fe/γ-Al_2O_3 surface is due to the greater conversion efficiencies, as highlighted by the higher concentrations of all gaseous species, and (b) with steam, wherein in addition to the greater accumulation of coke on the iron catalyst, the carbonaceous structure of the compared AK catalyst can be involved in steam reforming reactions, generating a partial consumption of its mass. A test under the extreme

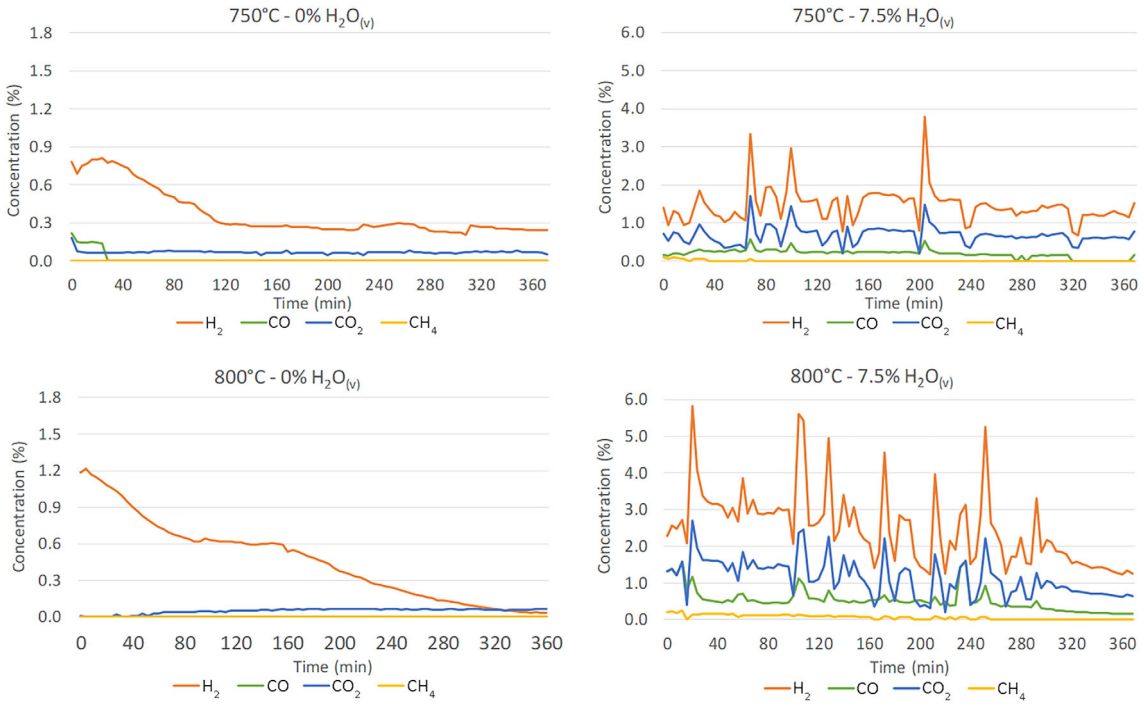

FIGURE 2 Time evolution of main gas concentrations during tests with Fe/γ-Al_2O_3, under different operating conditions

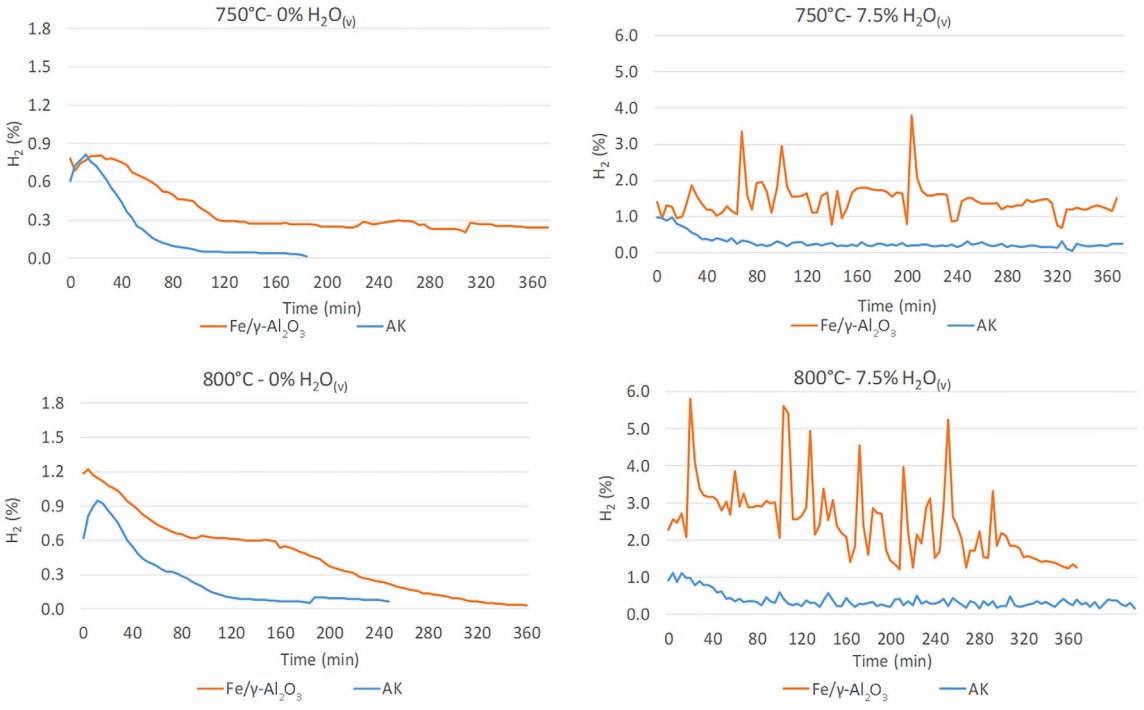

FIGURE 3 Time evolution of hydrogen concentration during tests with Fe/γ-Al_2O_3 and activated carbon (AK), under different operating conditions

operating conditions (800°C–7.5% H_2O) without naphthalene was carried out to verify whether the AK could be consumed by WG reaction (Figure 5). The production of H_2 and CO is low (mainly due to the WG reaction) but leads to a mass variation $\Delta_{wt.} = -0.7$ mg/min. With naphthalene, this variation is more than counterbalanced by the coke accumulation, with a final $\Delta_{wt.} = +0.51$ mg/min.

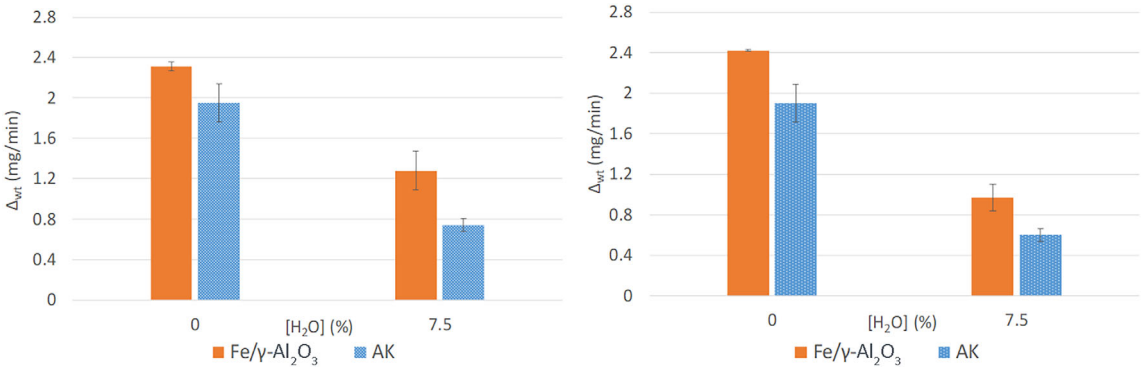

FIGURE 4 Variation of catalysts mass after the experimental tests at 750°C (left) and 800°C (right). AK, activated carbon

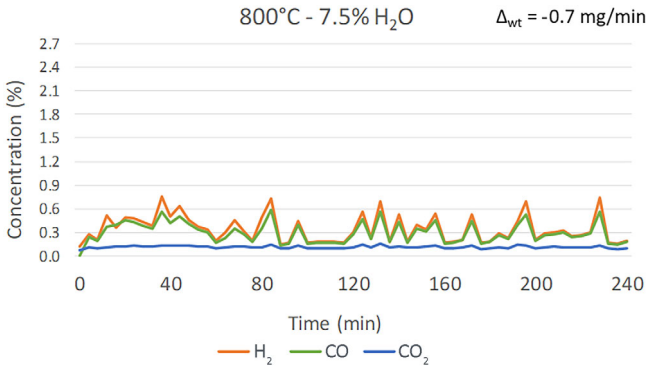

FIGURE 5 Time evolution of H_2, CO, and CO_2 concentration in activated carbon (AK) test at 800°C and 7.5% of steam without naphthalene

3.3 | Naphthalene conversion efficiencies

The naphthalene conversion efficiency was evaluated using Equation (2):

$$X_{C_{10}H_8} = \frac{(C_{10}H_8)_{IN} - (C_{10}H_8)_{OUT}}{(C_{10}H_8)_{IN}} \quad (2)$$

where $(C_{10}H_8)_{IN}$ is the concentration of naphthalene fed into the reactor, and $(C_{10}H_8)_{OUT}$ is the concentration of naphthalene sampled at different times at the reactor exit, both measured in terms of mol_{C10H8}/L_N. The results are reported in Figure 6. The AK, probably due to the high specific surface area, allows to obtain conversion efficiencies close to 100% in the first 5 min. Immediately after, however, its activity is reduced until it becomes inefficient enough to guarantee an adequate cleaning of the carrier gas containing naphthalene. On the contrary, Fe/γ-Al_2O_3 shows a more stable trend.

At 750°C for the Fe/γ-Al_2O_3 and at 800°C for both catalysts, the steam leads to enhanced removal performance. This is due to the WG, WGS, and steam reforming reactions. They remove part of the coke that is deposited on the active sites, determining a reduction in the catalyst mass gain, a greater production of H_2, CO, and CO_2, and an increase in conversion efficiencies. The higher removal of coke in tests with Fe/γ-Al_2O_3 compared to that obtained with AK was confirmed by a porosimetric analysis carried out on samples taken at the end of tests at 750°C. For the AK, even in the presence of steam, it was measured a reduction of more than 83% of the specific surface area compared to that of the fresh AK. For the iron-based alumina catalyst, the reduction was only 26.4% and 13.5% in the tests without and with steam, respectively.

3.4 | SEM-EDX analysis

The SEM-EDX analyses were performed to examine the morphology, structure variation, and surface composition of the tested catalysts. An X-ray diffraction (XRD) analysis was also performed only on the γ-Al_2O_3 samples, before and after their iron treatment, with the aim to check the homogeneity of the iron doping process on the support surface (Figure 7). The SEM analysis of untreated γ-Al_2O_3 and Fe/γ-Al_2O_3 shows that the iron oxide produces some clusters due to its precipitation (Figure 7). Nevertheless, the XRD analysis (Figure 7 right side) does not show significant differences between γ-Al_2O_3 and Fe/γ-Al_2O_3, confirming that the observed clusters do not affect the iron distribution. Furthermore, as defined by the porosimetric data, the support shows no signs of alteration or damage due to the iron doping treatment. This is a crucial factor since the metal should be well dispersed to improve the catalytic reaction, and it should not cause any contamination or react with the catalyst support.[27]

After all the experimental tests, with and without steam, the Fe/γ-Al_2O_3 appeared completely black due to the coke deposition on the surface, as already confirmed by the data of bed mass increase. SEM analysis and a mapping of the elements C, Al, Fe, and O that are present

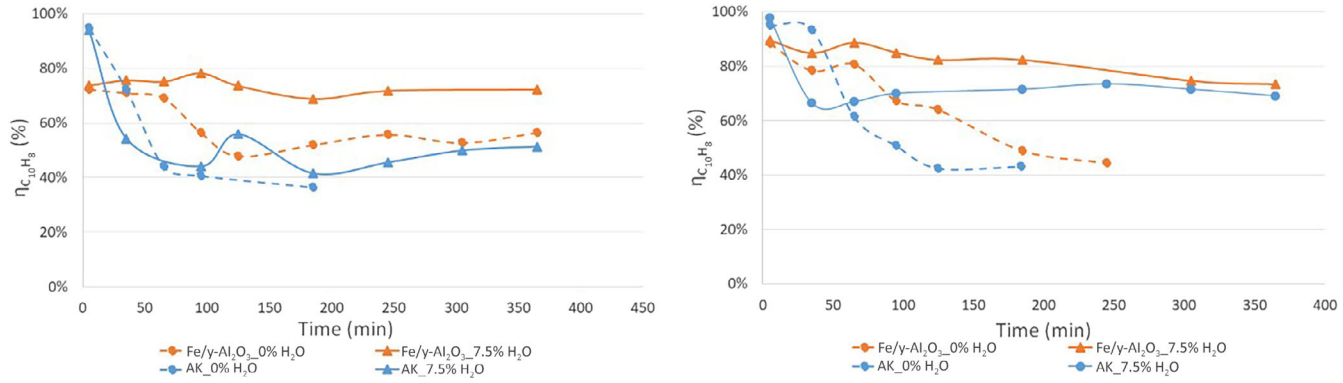

FIGURE 6 Naphthalene conversion efficiencies for the tests with Fe/γ-Al_2O_3 and activated carbon (AK), at 750°C (left) and 800°C (right), without and with steam

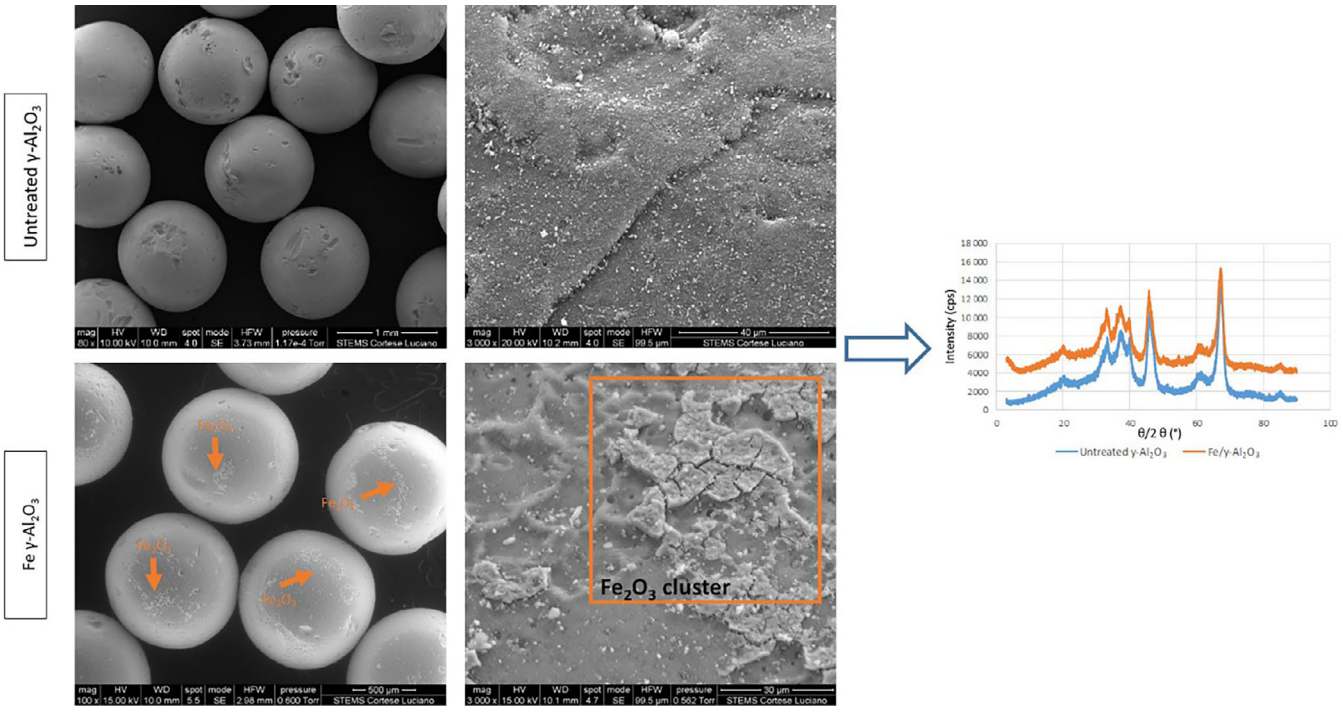

FIGURE 7 Scanning electronic microscopy (SEM) images of the untreated γ-Al_2O_3 and fresh Fe/γ-Al_2O_3 spheres at different magnifications (from left: 100× and 3000×) and XRD analysis. XRD, X-ray diffraction; WD, working distance; HV, high voltage; HFW, horizontal field width

on the surface were also carried out to analyze the catalyst and coke morphological characteristics. Although this type of analysis may be unrepresentative when performed on small areas of a sample at high magnifications,[11] it can provide some useful insight. In all the SEM photographs shown in Figure 8, the iron clusters appear clearly visible, identified by the mapping of the carbon and iron compounds. The mapping of the carbon element, after the naphthalene reforming reaction, shows that the analyzed surface is completely covered by coke. It is worth mentioning that the overlay image of all the elements detected by the EDX analysis is clearly influenced by the aluminum of the support. This indicates that the thickness of the carbon layer is lower than 2 μm (which is the thickness within which the FEI Inspect™ S50 Scanning Electron Microscope detects all the present elements) and that, therefore, the concentration of aluminum prevails over all other elements. Nonetheless, such a carbon layer, although extremely thin, is sufficient to cover the active sites and to partially deactivate the catalyst.

The AK catalysts were also analyzed, and the surface elements were mapped by the SEM-EDAX analysis (Figure 9). Only the mapping of all the elements for the conditions at 750°C without and with steam is reported since no significant variations were detected when the

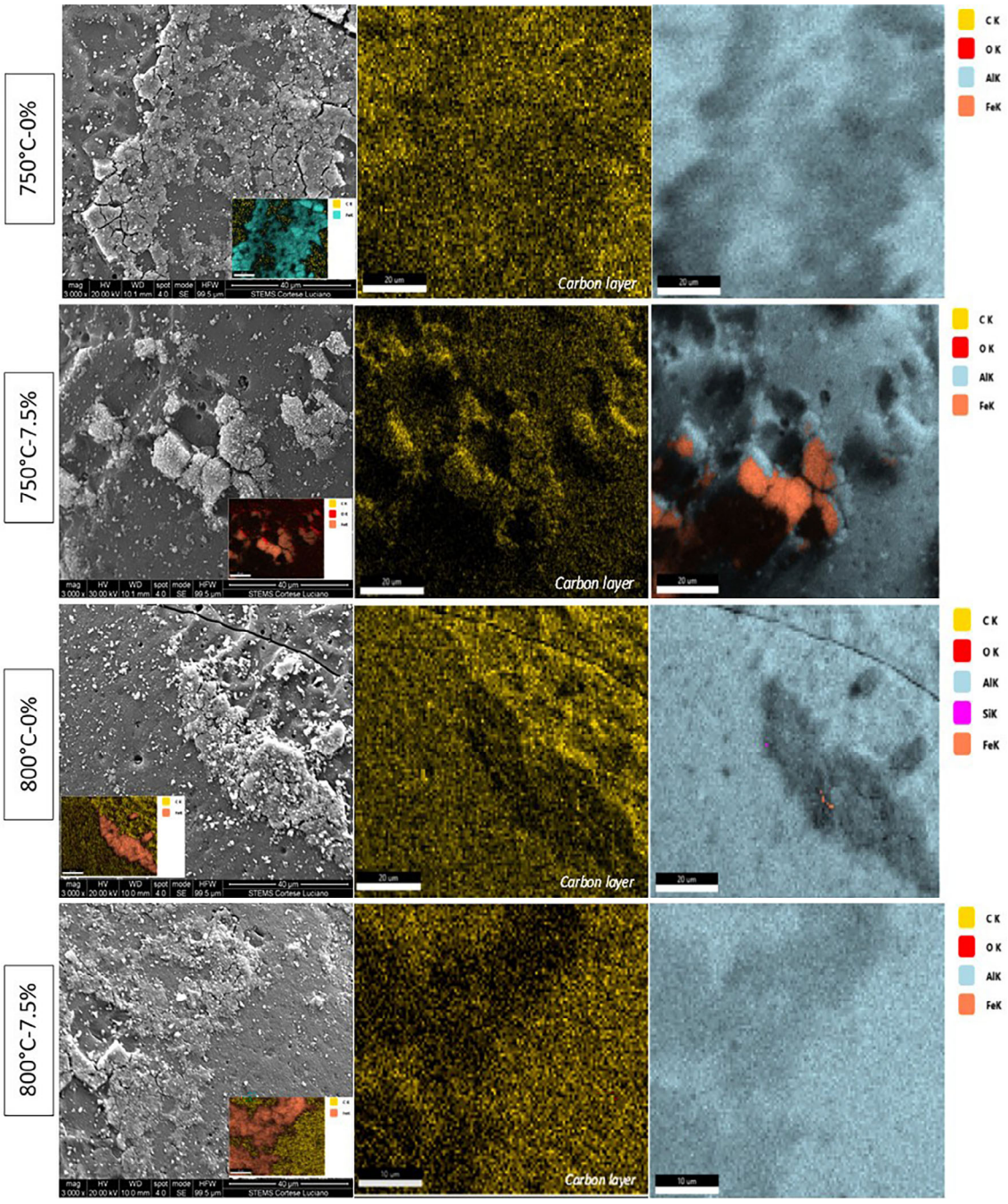

FIGURE 8 Scanning electronic microscopy (SEM) images of the Fe/γ-Al_2O_3 spheres, under different operating conditions, at 3000× magnification, carbon mapping images and element mapping images of C, O, Al, and Fe. WD, working distance; HV, high voltage; HFW, horizontal field width

temperature increased. The extremely heterogeneous nature of AK and its carbonaceous nature, similar to the produced coke, clearly prevents distinguishing possible differences. The overlay mapping of all the detected elements makes clear the heterogeneity of the inorganic composition, even after the naphthalene reforming reactions. Indeed, in several areas, O, Na, Mg, Al, Si, Ca, and Fe are still predominant compared to the carbon of both AK and coke. However, this carbon, although present in an extremely thin layer (<2 μm) is sufficient to reduce the initial high conversion efficiencies and is able to deactivate the AK catalyst.

3.5 | Raman spectroscopy analysis

A Raman spectroscopy analysis of the samples was performed on the catalyst granules before and after the

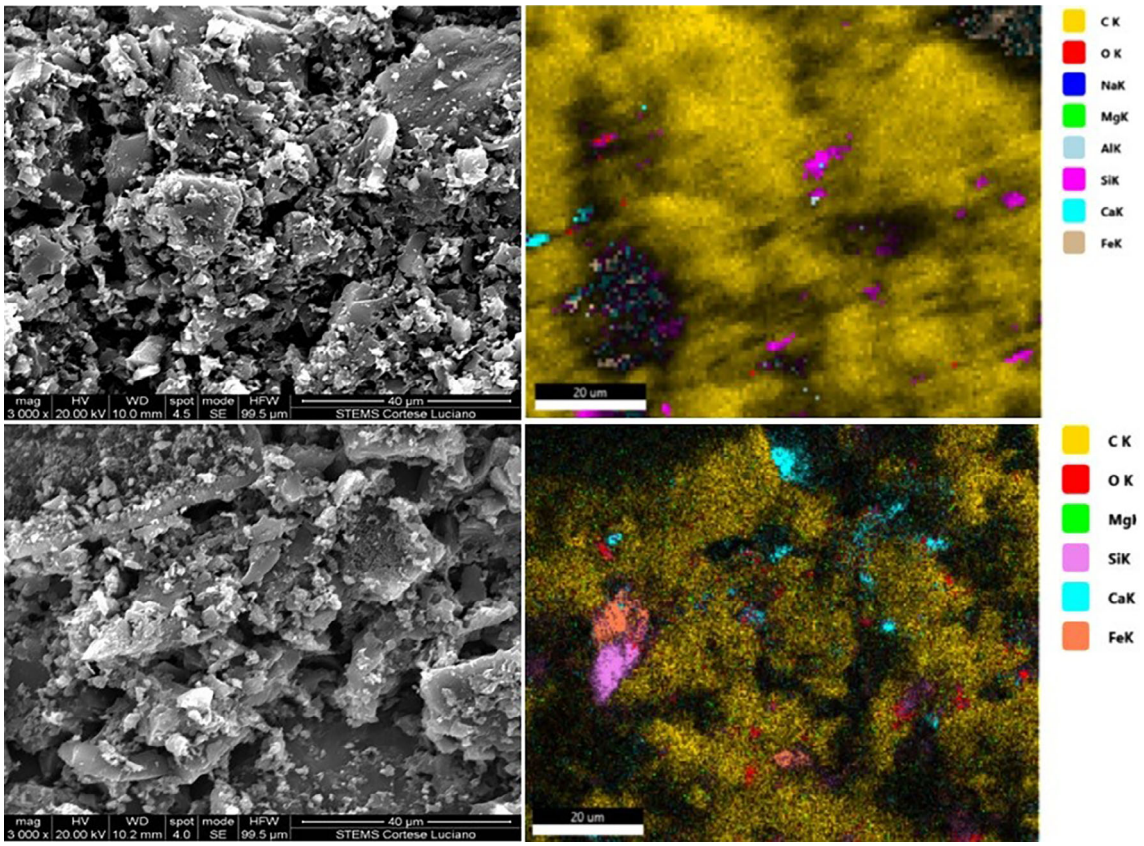

FIGURE 9 Scanning electronic microscopy (SEM) images of the activated carbon (AK) granules tested at 750°C without (top) and with steam (bottom) at 3000× magnification and element mapping images. WD, working distance; HV, high voltage; HFW, horizontal field width

naphthalene cracking tests to further study the nature of the coke layer and to assess its reactivity and the catalyst deactivation mechanism. The main Raman spectra obtained for each catalyst, before and after the naphthalene cracking test, without and with steam, are reported in Figure 10. It is worth mentioning that, for the AK catalyst, which already presents a carbon structure, all the Raman spectra present very similar spectral features with respect to the produced carbon deposits—both being characteristics of disordered carbon materials. The presence and the characteristics of the carbon deposits generated as by-products of the naphthalene cracking/reforming reactions can be clearly seen for the Fe/γ-Al_2O_3, shown in the lower panels of Figure 10B.

For all the catalysts, the typical Raman spectrum of highly disordered/amorphous carbons can be detected. The carbon is characterized by two well-known bands, namely, the D band (or disorder band), at ∼1350 cm^{-1}, activated by the presence of defects within the carbon material, and the G band (or graphite band), at ∼1580 cm^{-1}, attributed to the existence of a graphitic component. Details on the physical origin of these two Raman modes can be found elsewhere.[36,37] Although the relative intensity of the two bands, or the $I(D)/I(G)$ ratio, is often used to assess the graphitization degree of the defective/amorphous carbon materials,[36,37] considering the non-monotonic trend of this ratio as a function of the graphitization degree of the carbon structure,[36–39] other parameters must be taken into account when comparing similar Raman spectra. These are the width of the D and G bands or the intensity of the intermediate spectral valley region between the two bands (i.e., the spectral region between ∼1400 and ∼1550 cm^{-1}).[40] As noticed and discussed in our recent work,[23] the Raman spectra resulting from tests with naphthalene, indicated the formation of a carbon deposit whose carbon structure is highly disordered/amorphous (as shown in part A of Figure 10). Indeed, the Raman spectrum of the carbon deposit grown on the AK granules during the naphthalene test presents a slight broadening of the D and G bands together with a clear increase in the spectral valley region, as compared to the spectrum of the fresh/pristine AK. This observed increase in the region between the D and G bands may be related to an increase in the amorphous component of the carbon material, and it is typically referred to as D3 disorder band (∼1500 cm^{-1}).[41] Such an increase, together with a modest increase in the lateral spectral regions, particularly in the 1100–1250 cm^{-1} region, is indicative of a higher index of disorder of carbon structures when operating the systems with

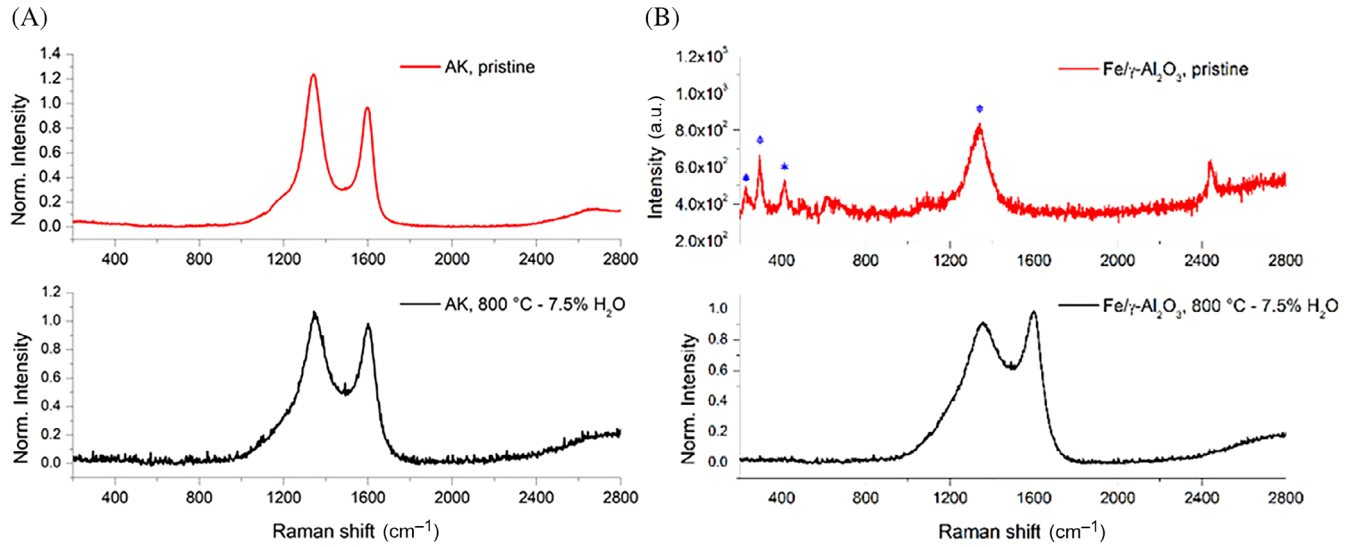

FIGURE 10 Raman spectra comparisons of the untreated (top) catalysts and post reaction catalysts (bottom): (A) activated carbon and (B) Fe/γ-Al_2O_3. Symbols (*) refer to the Raman bands of Fe contribution to the catalyst, and symbols (+) refer to the γ-A_2O_3 component. AK, activated carbon

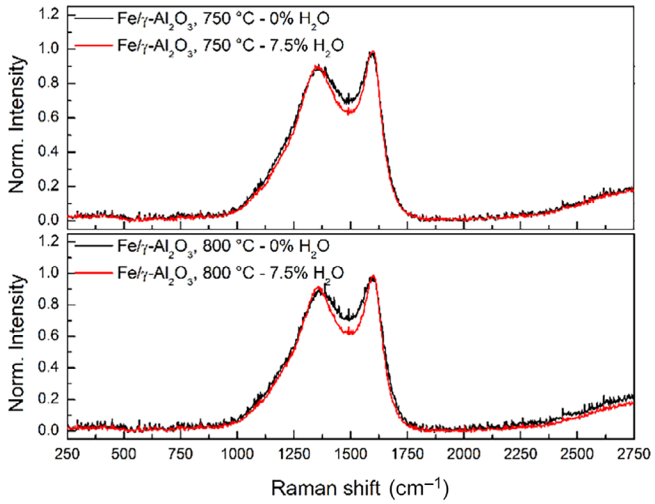

FIGURE 11 Raman spectra of the Fe/γ-Al_2O_3 after the cracking/reforming test with naphthalene at 750 and 800°C, without and with steam

naphthalene as compared to the carbon structure of the pristine AK. Nevertheless, such an amorphous character of the carbon deposits is more clearly observable from the Fe/γ-A_2O_3 measurements. For the latter, indeed, the presence and the exact nature of the carbon deposits can be inferred by the absence of carbon in the pristine catalysts: therefore, the whole spectrum can be attributed to the produced coke (as shown in side B of Figure 10). These spectra closely resemble, for instance, the typical Raman spectra of the highly disordered flame-formed nascent soot particles,[42] or those obtained from pyrolyzed wood, particularly when operating at low heat treatment temperatures.[40] A comparison of the Raman spectra of the Fe/γ-A_2O_3 catalysts used for naphthalene cracking, without and with steam, is reported in Figure 11. The temperature effect is negligible, while the carbon deposit in the presence of steam appears relatively more graphitic than that obtained in the absence of steam, based on the observed reduction of the valley region (~1500 cm^{-1}) when operating with steam. The same trend can be observed for both the temperatures of 750 and 800°C. It is likely that, during the oxidation stage, the effect of steam in removing the carbon deposit is more effective towards the more amorphous and less ordered component of the carbon deposits, thus ultimately leading to a slightly more graphitic carbon residue.

4 | CONCLUSIONS

The study compared the naphthalene removal efficiency of two different catalysts, a Fe/γ-Al_2O_3 and an AK, in a series of long-term tests under different conditions of temperature (750 and 800°C) and steam concentration (0% and 7.5%). The coke deposits formed on the surfaces of both the catalysts were studied. The deposit formed on the AK has the same carbonaceous nature as the catalyst, thus complicating an accurate characterization. The use of a non-carbonaceous catalyst makes the structure of the coke produced easily distinguishable and can provide useful insights into its reactivity.

The results showed that the AK catalyst displays a removal efficiency close to 100% in the initial stages of the tests. This could be due to its high specific surface area (928 m^2/g) compared to that of Fe/γ-Al_2O_3 (150–

170 m^2/g). However, after only 30 min, the coke deposits cause gradual deactivation, which leads this catalyst to be less performing in the long term than the iron-based catalyst. The latter, in the presence of steam, seems to enhance the reactions of WG and WGS, determining a higher CO and H_2 production and a lower coke accumulation.

Coke buildup was detected under all the operating conditions tested, ultimately also inhibiting the performance of Fe/γ-Al_2O_3 catalyst by deactivation.

All the catalyst samples were analyzed by SEM-EDX and Raman spectroscopy. The mapping of the elements in the SEM-EDX analysis of Fe/γ-Al_2O_3 suggests that the surface of the alumina was completely covered by a carbon layer. This layer, albeit extremely thin (<2 μm), was further analyzed by Raman spectroscopy. The results showed that there are no detectable differences between coke produced at two different temperatures, while the absence or the presence of steam could create different coke layer buildups. The steam, indeed, easily reacts with the more amorphous components of the coke layer, while the less amorphous carbon sticks to the surface of the catalysts, even under the extreme conditions tested at 800°C and 7.5% steam. This would make it necessary to operate at even higher temperatures and steam concentrations to reduce the coke-induced deactivation of the catalysts and ensure high performance for long-term operation.

NOMENCLATURE

List of acronyms and symbols

AK	activated carbon
BET	Brunauer–Emmett–Teller
DFT	density functional theory
EDX	energy-dispersive X-ray analysis
GC-MS	gas chromatograph-mass spectrometer
GC-TCD	gas chromatograph-thermal conductivity detector
SEM	scanning electronic microscopy
WG	water–gas
WGS	water–gas shift
λ	wavelength

AUTHOR CONTRIBUTIONS

Francesco Parrillo: Conceptualization; data curation; investigation; methodology; software; writing – original draft; writing – review and editing. **Carmine Boccia:** Data curation; formal analysis; investigation; visualization; writing – original draft. **Giovanna Ruoppolo:** Data curation; formal analysis; investigation; software. **Mario Commodo:** Data curation; formal analysis; investigation; software; writing – original draft. **Franco Berruti:** Data curation; formal analysis; writing – review and editing. **Umberto Arena:** Conceptualization; data curation; methodology; supervision; validation; writing – review and editing.

ACKNOWLEDGEMENTS

The authors greatly appreciated the contributions of Miss Ilaria Abbate and Mr. Domenico Tedesco for their contributions in carrying out the experimental tests. The authors also wish to thank Mr. Luciano Cortese for his technical assistance in SEM-EDX observations. Open Access Funding is provided by Universita degli Studi della Campania Luigi Vanvitelli within the CRUI-CARE Agreement.

PEER REVIEW

The peer review history for this article is available at https://publons.com/publon/10.1002/cjce.24535.

DATA AVAILABILITY STATEMENT

Data available on request from the authors.

REFERENCES

[1] U. Arena, in *Fluidized-Bed Technologies for Near Zero Emission Combustion and Gasification* (Ed: F. Scala), Woodhead Publishing, Sawston, UK **2013**, Ch.17.
[2] N. Mahinpey, A. Gomez, *Chem. Eng. Sci.* **2016**, *148*, 14.
[3] C. Courson, K. Gallucci, in *Substitute Natural Gas from Waste: Technical Assessment and Industrial Applications of Biochemical and Thermochemical Processes* (Eds: M. Materazzi, P. U. Foscolo), Academic Press, Carmbidge, MA **2019**, Ch.8.
[4] X. Zeng, Y. Ueki, R. Yoshiie, I. Naruse, F. Wang, Z. Han, G. Xu, *Carbon Resour. Convers.* **2020**, *3*, 1.
[5] J. Ashok, N. Dewangan, S. Das, P. Hongmanorom, M. H. Wai, K. Tomishige, S. Kawi, *Fuel Process. Technol.* **2020**, *199*, 106252.
[6] J. R. H Ross, *Heterogeneous Catalysis*, Elsevier, Amsterdam, The Netherlands **2012**.
[7] N. B. Klinghoffer, M. J. Castaldi, A. Nzihou, *Ind. Eng. Chem. Res.* **2012**, *51*(40), 13113.
[8] G. Zhang, A. Su, Y. Du, J. Qu, Y. Xu, *J. Colloid Interface Sci.* **2014**, *433*, 149.
[9] G. Ravenni, Z. Sàrossy, J. Ahrenfeldt, U. B. Henriksen, *Renewable Sustainable Energy Rev.* **2018**, *94*, 1044.
[10] J. Ren, J. P. Cao, X. Y. Zhao, Y. L. Liu, *Fuel Process. Technol.* **2021**, *216*, 106782.
[11] H. Marsh, F. Rodriguez-Reinoso, *Activated Carbon*, 1st ed., Elsevier, Oxford, UK **2006**.
[12] D. M. L. Griffiths, J. S. R. Mainhood, *Fuel* **1967**, *46*, 167.
[13] Z. El-Rub, E. A. Bramer, G. Brem, *Fuel* **2008**, *87*, 2243.
[14] S. Hosokai, K. Kumabe, M. Ohshita, K. Norinaga, C. Z. Li, J. I. Hayashi, *Fuel* **2008**, *87*, 2914.
[15] S. Hosokai, K. Norinaga, T. Kimura, M. Nakano, C. Z. Li, J. I. Hayashi, *Energy Fuels* **2011**, *25*, 5387.
[16] P. N. Bhandari, A. Kumar, D. D. Bellmer, R. L. Huhnke, *Renewable Energy* **2014**, *66*, 346.
[17] F. Nestler, L. Burhenne, M. J. Amtenbrink, T. Aicher, *Fuel Process. Technol.* **2016**, *145*, 31.
[18] F. Parrillo, G. Ruoppolo, U. Arena, *Energy* **2020**, *190*, 116385.

[19] F. Di Gregorio, F. Parrillo, E. Salzano, F. Cammarota, U. Arena, *Chem. Eng. J.* **2016**, *291*, 244.
[20] D. Fuentes-Cano, F. Parrillo, G. Ruoppolo, A. Gómez-Barea, U. Arena, *Fuel Process. Technol.* **2018**, *172*, 125.
[21] L. Liu, M. Paskevicius, H. Wang, G. Parkinson, J. Veder, X. Hu, C. Li, *Fuel* **2019**, *253*, 441.
[22] J. R. Rostrup-Nielsen, *Catalytic Steam Reforming*, Springer, Heidelberg, Germany **1984**.
[23] C. Boccia, F. Parrillo, G. Ruoppolo, M. Commodo, F. Berruti, U. Arena, *Fuel Process. Technol.* **2021**, *141*, 31.
[24] A. Ochoa, J. Bilbao, A. G. Gayubo, P. Castano, *Renewable Sustainable Energy Rev.* **2020**, *119*, 109600.
[25] J. C. Védrine, *Metal Oxides in Heterogeneous Catalysis*, Elsevier, Amsterdam, The Netherlands **2018**.
[26] B. Pawelec, in *Metal Oxides, Chemistry and Application* (Ed: J. L. C. Fierro), CRC Taylor & Francis, Boca Raton, FL **2006**.
[27] B. Ramadhani, T. Kivevele, J. H. Kihedu, Y. A. C. Jande, *Biomass Convers. Biorefin.* **2020**, *12*, 1369.
[28] P. Munnik, P. E. de Jongh, K. P. de Jong, *Chem. Rev.* **2015**, *115*(14), 6687.
[29] R. Prins, *J. Catal.* **2020**, *392*, 336.
[30] J. Cummings, *Kirk-Othmer Concise Encyclopedia of Chemical Technology*, 5th ed., Wiley-Interscience, New York **2007**.
[31] R. Coll, J. Salvadò, X. Farriol, D. Montané, *Fuel Process. Technol.* **2001**, *74*, 19.
[32] J. Meng, Z. Zhao, X. Wang, J. Chen, A. Zhen, Z. Huang, G. Wei, H. Li, *J. Energy Inst.* **2019**, *92*, 1765.
[33] U. Arena, L. Zaccariello, M. L. Mastellone, *Waste Management* **2010**, *30*, 1212.
[34] U. Arena, F. Di Gregorio, *Fuel* **2014**, *117*, 528.
[35] F. Miccio, A. Picarelli, G. Ruoppolo, *Fuel Process. Technol.* **2016**, *141*, 31.
[36] A. C. Ferrari, J. Robertson, *Phys. Rev. B* **2001**, *64*, 075414.
[37] L. G. Cançado, A. Jorio, E. H. Martins Ferreira, F. Stavale, C. A. Achete, R. B. Capaz, M. V. O. Moutinho, A. Lombardo, T. S. Kulmala, A. C. Ferrari, *Nano Letters* **2011**, *11*, 3190.
[38] A. Merlen, J. G. Buijnsters, C. Pardanaud, *Coatings* **2017**, *2017*(7), 153.
[39] P. Minutolo, M. Commodo, A. Santamaria, G. De Falco, A. D'Anna, *Carbon* **2014**, *68*, 138.
[40] M. W. Smith, I. Dallmeyer, T. J. Johnson, C. S. Brauer, J. S. McEwen, J. F. Espinal, M. Garcia-Perez, *Carbon* **2016**, *100*, 678.
[41] A. Sadezky, H. Muckenhuber, H. Grothe, R. Niessner, U. Poschl, *Carbon* **2005**, *43*, 1731.
[42] M. Commodo, G. De Falco, P. Minutolo, A. D'Anna, *Fuel* **2018**, *216*, 456.

How to cite this article: F. Parrillo, C. Boccia, G. Ruoppolo, M. Commodo, F. Berruti, U. Arena, *Can. J. Chem. Eng.* **2022**, 1. https://doi.org/10.1002/cjce.24535